Available online at www.sciencedirect.com
ScienceDirect
Journal of Power Sources 172 (2007) 57–66
JOURNAL OF POWER SOURCES
www.elsevier.com/locate/jpowsour

The relationship between proton conductivity and water permeability in composite carboxylate/sulfonate perfluorinated ionomer membranes

Jesse E. Hensley *, J. Douglas Way [1]

Colorado School of Mines, Department of Chemical Engineering, 1613 Illinois Street, Golden, CO 80401, USA

Received 6 October 2006; received in revised form 27 November 2006; accepted 11 December 2006
Available online 16 December 2006

Abstract

Composite carboxylate/sulfonate Nafion® films were prepared with different ratios of anion equivalents as a test of the relationship between proton conductivity and water permeability in perfluorinated ionomers. Substitution of carboxylate groups for sulfonate groups dramatically reduced water permeability and modestly reduced proton conductivity in the films. Small angle X-ray scattering (SAXS) was used to probe the polymer microstructure and showed that with up to 20% carboxylate equivalents, the size of hydrated ionic domains within the ionomer remains constant. Water sorption measurements showed little decrease in water uptake with increased carboxylate functionality, supporting the SAXS data. Methanol/water permeability experiments showed that the carboxylate moieties slow the diffusion of both water and methanol, with no permselectivity of water. Results indicate that the proton transport mechanism is altered by addition of carboxylic acid. As such, the composites may show interesting behavior in H_2/O_2 and direct methanol fuel cells. It is proposed that permeability and conductivity measurements may provide an inexpensive and simple screening tool for early evaluation of new experimental proton exchange membranes.

Keywords: Composite membrane; Proton conductivity; Water permeability; DMFC; Carboxylate ionomer; Sorption

1. Introduction

Perfluorinated ionomers are widely studied for use as polymer electrolyte membrane (PEM) materials in low temperature hydrogen fuel cells and direct methanol fuel cells (DMFCs). In particular, the Nafion® membranes, produced by DuPont, and similar perfluorosulfonic acid ionomers manufactured by Dow and Asahi Glass, have drawn significant attention. These materials require continuous hydration to maintain high proton conductivity in H_2/O_2 fuel cells, a condition that is difficult to achieve, especially when operating above 100 °C. Further, these materials do not provide a sufficient barrier to methanol permeation, resulting in power and fuel losses in the DMFC [1–4]. Since electrode kinetics are enhanced and since catalyst poisoning is less severe above 100 °C in H_2/O_2 fuel cells, there is a great interest in PEM materials that can maintain high proton conductivity at elevated temperatures [5–7]. And, to reduce or eliminate methanol crossover in DMFCs, PEM materials with decreased methanol permeability and high proton conductivity are especially desired [8–10].

In principle, both problems could be solved with an electrolyte that allows rapid transport of protons through its bulk while being impermeable to water and methanol. Unfortunately, efficient proton conduction in modern PFSAs is dependent on water to act as a 'bridge' or carrier between covalently bound anionic moieties. A logical step toward water independence will be to develop PEM materials that require less water for high proton conductivity, and/or to develop materials that do not rely on highly mobile water for proton conduction. Researchers have approached the issue of coupled water and proton transport in many ways, including incorporation of fillers or dopants in the polymer matrix to enhance proton conduction at high temperatures and low membrane water content [7,11–15], and to reduce methanol permeation in the electrolyte [4,16–18]. Other methods include the copolymerization of functional additives with the polymer matrix to align conducting pathways, and the coupling of sulfonic acid functional groups with active sites in mesoporous ceramic materials to limit membrane swelling [19,20].

* Corresponding author. Tel.: +1 303 384 2017; fax: +1 303 273 3730.
E-mail addresses: jessehensley@alumni.nd.edu (J.E. Hensley), dway@mines.edu (J.D. Way).
[1] Tel.: +1 303 273 3519; fax: +1 303 273 3730.

0378-7753/$ – see front matter © 2006 Elsevier B.V. All rights reserved.
doi:10.1016/j.jpowsour.2006.12.014

Nomenclature

A	area (cm^2)
c	concentration (M)
d	size of scattering feature (Å)
D	diffusion coefficient ($m^2\,h^{-1}$)
EW	equivalent weight (g dry polymer per mole equivalents)
J	flux ($kg\,m^{-2}\,h^{-1}$)
l	thickness (cm)
L	distance between current-measuring electrodes (cm)
m	mass (g)
p	pressure (bar)
P	permeability ($kg\,m\,m^{-2}\,bar^{-1}\,h^{-1}$)
R	resistance (Ω)
s	magnitude of reciprocal lattice vector ($Å^{-1}$)
S	solubility ($kg\,m^{-3}\,bar^{-1}$)
t	time (h)
V	volume (L)

Greek letters

α	selectivity
θ	one-half the diffraction angle (°)
λ	water content (moles H_2O per mole equivalents)
Λ	X-ray wavelength (Å)
σ	conductivity ($S\,cm^{-1}$)

Subscripts

d	dry
H_2O	water
MeOH	methanol
OH^-	aqueous alkali hydroxide
p	permeate
w	wet
x	cross-sectional

Superscripts

$'$	feed
$''$	permeate

In general, the goals of these research activities are to increase the structural order of water in the PEM, to increase the water uptake by the polymer, to hold water in place within the ionomer, or to shorten the path the protons must take to permeate the membrane.

For researchers involved in the development of these improved PEM materials, it will be important to know how the transport of protons is affected by membrane modification, and how it differs from conduction in the unmodified PFSAs. It is now well established that when fully hydrated, protons diffuse through Nafion® and Nafion®-like membranes by two mechanisms: along fixed sulfonic acid sites and structured water molecules by a Grotthuss or "hopping" mechanism and as hydrated ions, the so-called "vehicle mechanism" [6,8,21]. It is thought that the Grotthuss mechanism plays a larger role in proton conductivity in highly water-swollen sulfonic acid based ionomers [22,23], yet experimental evidence shows that the electroosmotic drag coefficient, or number of water molecules co-transported with each conducting proton, increases as membrane water content increases [22,24,25]. Furthermore, it is known that as PFSAs swell (increase in water content), both the self-diffusion coefficient of water within the membrane and the proton conductivity increase in kind [26–28]. Therefore, this strongly suggests that water and proton transport in hydrated Nafion® films are linked, and that performance in both areas is dependent on the polymer's chemical structure and/or morphology.

Based on the above commentary, a membrane that allows high proton conductance via the Grotthuss mechanism *only* is highly desirable [5,7,13]. In such a film, one might expect high conductance with little to no water permeance. In improved PEM materials, an obvious criterion for enhanced fuel cell performance is high proton conduction at high temperatures and lowered relative humidity. Few researchers go beyond this criterion before further testing the membranes in a fuel cell environment, however, when in fact the conductivity test will not give insight into the relative contribution of Grotthuss proton hopping. If the dominant proton conduction mechanism in the film requires highly mobile water for "vehicle"-type proton movement, the membrane will likely dry out in fuel cell operation due to electroosmotic drag of water, regardless of the performance in static conductivity tests. Therefore, measurement of the long-range mobility of water within the membrane may be as important as the measurement of bulk conductivity when screening new electrolyte materials.

In this paper, we investigated the relationship between proton conductivity and water permeability in composite carboxylate/sulfonate Nafion® membranes. Since the carboxylic acid form of Nafion® is known to exhibit lower water permeability than the sulfonic acid form [29], water permeability can be adjusted by changing the ratio of carboxylate and sulfonate terminated side chains in a film. In testing these films, we can hypothesize whether the substitution of a fraction of the sulfonic acid in Nafion® with a weaker acid can offer any advantages in the fuel cell PEM.

2. Experimental

2.1. Materials

Nafion® 117, 115, 112, 111, and sulfonyl fluoride-form 111-F precursor films (1100 EW and 178, 127, 51, 25, and 25 μm thick, respectively) were purchased from Ion Power, Inc. or the Electrosynthesis Company, Inc. An additional lot of Nafion® 111-F precursor was provided by DuPont Fuel Cells. All films were subjected to an identical pretreatment before testing, consisting of a 24 h soak in room temperature distilled water, followed by refluxing for 2 h in 3% H_2O_2, 4 h in 1 M HNO_3, and 4 h in three fresh charges of 18 MΩ water. All films were stored in 18 MΩ water in sealed vials.

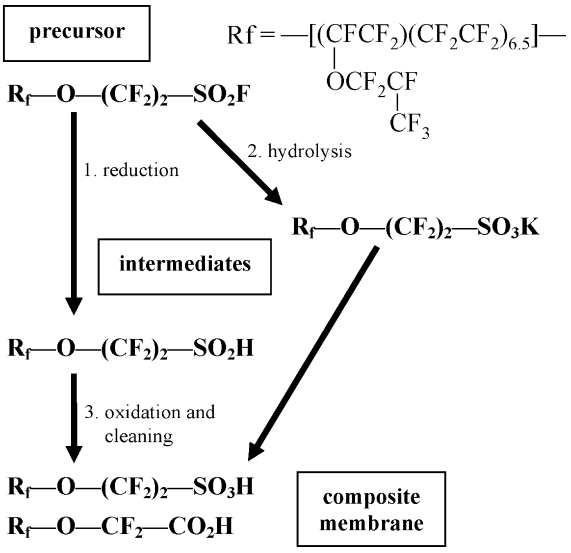

Fig. 1. Composite carboxylic acid/sulfonic acid membrane synthesis procedure.

2.2. Composite membrane synthesis

Nafion® films with both carboxylate and sulfonate terminated side chains were made using an adaptation of a procedure developed by Grot et al. [30]. The general procedure for making these films is shown in Fig. 1. Nafion® 111-F films were contacted with 48% (w/w) aqueous hydrazine for varying lengths of time to reduce sulfonyl fluoride to sulfinic acid. Films were then quenched in HNO_3, rinsed with water, and hydrolyzed in 13% KOH, 30% dimethyl sulfoxide (w/w) in water for 2 h at 70 °C. Next, films were rinsed in water, soaked in 1 M HNO_3, and oxidized in oxygen-enriched water at 80 °C for 8 h. Oxidation desulfinates the polymer, leaving a carboxylic acid at the end of the side chains. Then, films were annealed for 3 h at 165 °C. Finally, films were cleaned, pretreated, and stored in 18 MΩ water. Composite membranes were named using the form: S.###.***.HL, where S indicates that both sides of the precursor sheet were contacted with hydrazine, ### is the reduction time in min, *** is either 75w or 100 indicating reduction in 75 or 100% (v/v) aqueous hydrazine, H indicates that the film was tested in the H^+ counterion form, and L indicates a large sheet (~160 cm^2).

A control membrane containing 100% sulfonic acid equivalents was made by hydrolyzing, acidifying, annealing, and cleaning/pretreating a precursor film. This membrane was named "hydrolyzed precursor" in the results that follow. The hydrolyzed precursor is chemically identical to Nafion® 111 and of the same thickness. All converted films were sampled with FTIR through their thickness in several locations to ensure complete conversion of sulfonyl fluoride, absence of impurities, and to confirm a uniform distribution of ionic groups across the membrane area. The composition of the films (percentage of carboxylate equivalents) was measured using X-ray fluorescence (XRF) and FTIR as explained elsewhere [31].

2.3. Equivalent weight (EW) analysis

All films were checked for EW (g dry polymer per mole equivalents). Pretreated membrane samples were soaked in two fresh charges of 2 M HCl for 20 min each followed by six fresh charges of 18 MΩ water for 15 min each. Then, samples were soaked in 2 M NaCl, titrated to a phenolphthalein endpoint with 0.01 M NaOH, washed with water, vacuum dried, and weighed. EW was calculated by

$$\mathrm{EW} = \frac{m_\mathrm{d}}{V c_{\mathrm{OH}^-}} - 22 \quad (1)$$

where m_d is the dry sample mass (g), V the volume of titrant (L), and c_{OH^-} is the titrant concentration (M). The constant term accounts for the difference in mass between the Na^+ and H^+ ion.

2.4. FTIR analysis

FTIR measurements were performed at room temperature using a Thermo-Nicolet Nexus 870 FTIR Spectrometer with a mercury cadmium telluride (MCT) or dueterated triglycine sulfate (DTGS) detector and KBr beamsplitter. Samples were vacuum dried for 24 h at room temperature prior to analysis. Measurements were performed in attenuated total reflectance (ATR) or transmission mode, sampling to a depth of ~1 μm below the surface or through the full thickness of the films, respectively.

Transmission measurements were made with the DTGS detector at resolution of 1 (two data points per wavenumber) for 64 scans over a spectral range of 4000–400 cm^{-1}. ATR measurements were made with the MCT detector and a KRS-5 crystal placed on top of the sample in a Specac ATR cell, at a resolution of 2 for 1024 scans from 4000 to 650 cm^{-1}. ATR spectra were corrected to account for the different penetration depths of different wavelengths of light using Thermo-Nicolet's Omnic software.

2.5. Water permeability measurements

Water permeability was measured using a pervaporation apparatus described elsewhere [29]. Membrane samples were placed in a membrane cell and water at 35 °C was circulated past one surface of the sample. Vacuum was applied to the opposite surface of the sample at an absolute pressure of 4.0 ± 0.5 mbar. Membrane samples were equilibrated under vacuum for 2 h after which permeate was collected for a known amount of time. The flux of water through the membrane was calculated using the following equation:

$$J = \frac{m_\mathrm{p}}{At} \quad (2)$$

where J is the flux (kg m^{-2} h^{-1}), m_p the total permeate mass (kg), A the membrane area (m^2), and t is the time of collection (h). Membrane permeability was calculated using the solution diffusion model developed by Wijmans and Baker [32]:

$$J = \frac{P}{l}(p' - p'') \quad (3)$$

where P is the permeability (kg m m^{-2} bar^{-1} h^{-1}), l the membrane thickness (m), p' the feed-side vapor pressure of water

(bar), and p'' is the permeate side pressure (bar). The solution diffusion model assumes constant pressure within the membrane, minimal swelling of the polymer, a linear gradient in water activity across the membrane thickness, and a phase change from liquid to gaseous water at the liquid/membrane interface. These assumptions may not hold for the Nafion/water system, however. Thomas et al. have studied the water profile in a Nafion® membrane under steady state pervaporation via *in situ* small angle neutron scattering experiments [33] and found that under liquid feed conditions, the membrane is fully wet for a large thickness adjacent to the feed liquid, then decreases sharply in water content near the membrane/vacuum interface. Since water permeability changes with water content in Nafion® [22,34–36], it is inappropriate to assume constant permeability through the membrane thickness. Further, it is incorrect to assume that swelling is moderate at the feed-side membrane interface since Nafion® swells by 33% or more in liquid water [24,37]. Therefore, the permeabilities reported in this study are *average* values, with nonlinear gradients existing across the membranes' thickness.

Permeability may be divided into contributions from diffusivity D ($m^2\,h^{-1}$) and solubility S ($kg\,m^{-3}\,bar^{-1}$) as shown in the following equation:

$$P = DS \tag{4}$$

2.6. Proton conductivity measurements

Proton conductivity was measured at room temperature and 100% relative humidity using the four-point AC impedance method and a conductivity cell similar in design to that used by Doyle et al. [38]. Membrane samples were placed in the cell so that electrical current was forced between film surfaces, as shown in Fig. 2. Samples were allowed to equilibrate a minimum of 24 h in the cell. AC impedance was measured with a Gamry Instruments PCH/75 potentiostat over a frequency range of 100 Hz–100 kHz with a perturbation voltage of 10 mV. Impedance spectra showed a slight capacitive component and were fit to resistor/capacitor model circuits using Gamry Echem Analyst software. Conductivity was calculated from the following equation:

$$\sigma = \frac{L}{A_x R} \tag{5}$$

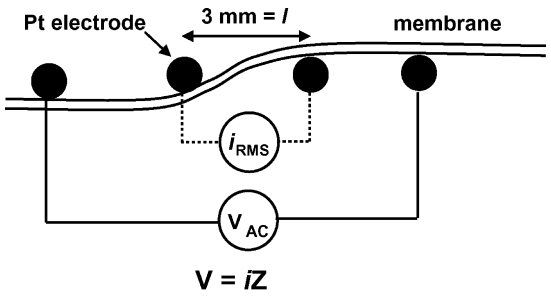

Fig. 2. Side view of membrane samples in conductivity measurements. Voltage is applied between the outer electrodes and current is measured between the inner electrodes. Impedance is calculated from the AC voltage and current values.

where σ is the membrane conductivity ($S\,cm^{-1}$), L the distance between current-measuring probes (cm), A_x the membrane cross-sectional area (cm^2), and R is the real part of the complex impedance (Ω). Conductivity values are reported as the average of separate measurements with an error of one standard deviation.

2.7. Methanol permeability and selectivity

Methanol permeability was measured using the pervaporation apparatus described in Section 2.5, with isothermal feed solutions of 1 or 2 M methanol. Total flux was calculated using Eq. (2). Methanol concentration in feed and permeate samples was measured using an Agilent Technologies 6850 gas chromatograph and 5973N mass spectral detector connected by a J&W Scientific DB-WAX capillary column. Water/methanol selectivity was calculated using the following equation:

$$\alpha = \frac{c''_{H_2O}/c''_{MeOH}}{c'_{H_2O}/c'_{MeOH}} \tag{6}$$

where α is the water/methanol selectivity, c_{H_2O} the concentration of water (M), c_{MeOH} the concentration of methanol (M), and the single and double prime superscripts indicate feed or permeate, respectively. Feed composition was taken as the arithmetic mean concentration of samples collected at the beginning and end of each experiment.

2.8. Water uptake

Water uptake was measured gravimetrically at room temperature with samples in the H^+ form. Samples were removed from water storage, patted dry, then quickly weighed and returned to storage. The wet (water swollen) mass was measured a minimum of four times, allowing the sample to soak in water for at least 30 min between measurements. The wet mass and error in measurement were taken as the average and standard deviation of the individual mass measurements. Membrane samples were then vacuum dried for 24 h and weighed. Dried H^+ form samples were assumed to contain one water molecule per equivalent as determined elsewhere [22] and the water uptake was calculated by

$$\lambda = \frac{EW(18m_d + EW(m_w - m_d))}{18(EW - 18)m_d} \tag{7}$$

where λ is the water content (moles H_2O per mole equivalents) and m_w is the mass of the water-swollen membrane (g).

2.9. SAXS

SAXS can be used to probe the sizes of phase-separated domains in Nafion® and has been demonstrated by many authors [39–42], so justification of the technique is not given here. Measurements were made with a Rigaku Rotaflex small angle X-ray instrument using a Cu Kα X-ray source at 8.05 kV and a He atmosphere. All samples were analyzed at room temperature. Two membrane pieces were placed side-by-side in a polyethy-

lene envelope with 30 μL of water and heat-sealed. A blank, water-filled envelope was measured for X-ray scattering, and the intensity subtracted from each measurement. All data was corrected for sample thickness. SAXS intensity was measured over the range $0.002 < s < 0.05$, where s is defined as

$$s = \frac{2\sin(\theta)}{\Lambda} \tag{8}$$

In Eq. (8), s is the magnitude of the reciprocal lattice vector ($Å^{-1}$), 2θ the diffraction angle, and Λ is the X-ray wavelength (1.54 Å for Cu Kα). The average size of the hydrophilic domains was estimated using Bragg's Law:

$$2d\sin\theta = \Lambda \tag{9}$$

where d is the size of the scattering feature ($Å^{-1}$). Combining Eqs. (7) and (8), an expression relating s to d was obtained:

$$d = \frac{1}{s} \tag{10}$$

3. Results

FTIR transmission spectra of Nafion® 111 and a representative composite membrane are shown in Fig. 3. Both spectra show a strong $–SO_3H$ stretch at ~1060 cm^{-1}, indicating that only a fraction of the sulfonyl fluoride groups in the precursor material are converted to carboxylic acid in the conversion process. The composite membrane shows a strong absorption band at 1785 cm^{-1} corresponding to the carbonyl stretch and a very weak absorption band at ~1450 cm^{-1} associated with the O–H stretch in CO_2H [43]. In comparison, Nafion® 111 shows no absorption bands associated with the carboxylic acid, a very strong H_3O^+ absorption [44] at ~1700 cm^{-1}, and a broad feature centered at 2210 cm^{-1} likely associated with water. Aside from these peaks, there are no contrasting features in the spectra at low wavenumbers, indicating that the conversion process successfully replaces a number of would-be sulfonic acid groups with carboxylic acid equivalents, with little to no formation of other bonds. There are subtle differences in the two spectra at high wavenumbers as well as obvious differences at 1700 and 2210 cm^{-1}, due to differences in the amount and nature of sorbed water in the membranes. This is an important result as it suggests a change in the chemical environment for water within the membranes. A detailed study of sorbed water in these films is beyond the scope of this work, but will be considered in later publications.

Table 1
Carboxylate content (percent carboxylic acid equivalents) and EW values for composite membranes

Membrane	[COOH] (mole CO_2^- / mole equivalents)	EW (g $mole^{-1}$)
Hydrolyzed precursor (i)	0	1120 ± 20
Hydrolyzed precursor (d)	0	1068 ± 23
Nafion 111	0	1102 ± 26
S020.75w.i	2.4 ± 0.3	1140 ± 25
S030.75w.d	4.4 ± 0.4	1134 ± 15
S040.75w.i	4.4 ± 0.4	1112 ± 24
S045.75w.d	5.1 ± 0.4	1158 ± 15
S060.75w.i	5.6 ± 0.4	1110 ± 24
S070.75w.i	7.5 ± 0.4	1126 ± 24
S065.75w.d	11.4 ± 0.5	1128 ± 24
S077.75w.d	17.6 ± 0.4	1144 ± 14
S095.75w.d	20.4 ± 0.3	1170 ± 17
S090.100.i	30.0 ± 0.2	1011 ± 12

The letters 'i' and 'd' indicate that the film was prepared using precursor film from Ion Power, Inc. or DuPont Fuel Cells, respectively.

Table 1 shows the equivalent weights of the composite membranes, along with hydrolyzed precursor and Nafion® 111 for comparison. It is apparent that the conversion process does not result in a loss of functional groups, and that different lots of precursor material give membranes with consistent ion exchange capacity. Furthermore, it is evident that Nafion® 111 purchased from the supplier and Nafion® 111 hydrolyzed from precursor do not differ significantly in ion exchange capacity.

Figs. 4 and 5 show comparative transmission and ATR spectra from a number of composite membranes. The transmission spectra show an evolution of the strong CO_2H peak at ~1785 cm^{-1} as the percentage of carboxylate groups increases, and a slight decrease in the intensity of the $–SO_3H$ stretch at

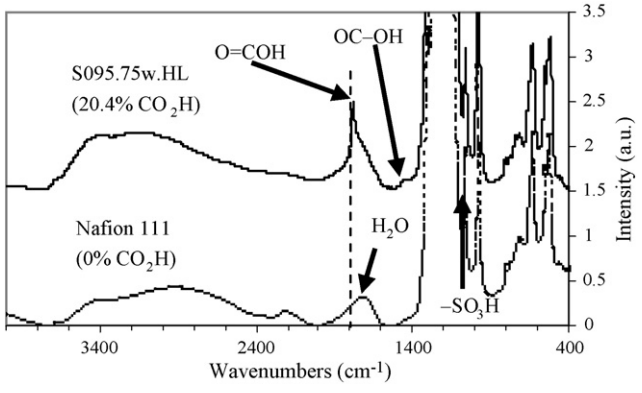

Fig. 3. FTIR spectra of vacuum dried composite membrane S095.75w.HL and Nafion® 111, both in H^+ counterion form. Measurements were taken in transmission mode, sampling the full thickness of the films. Spectra are stacked for comparison and the dashed line is added to guide the eyes.

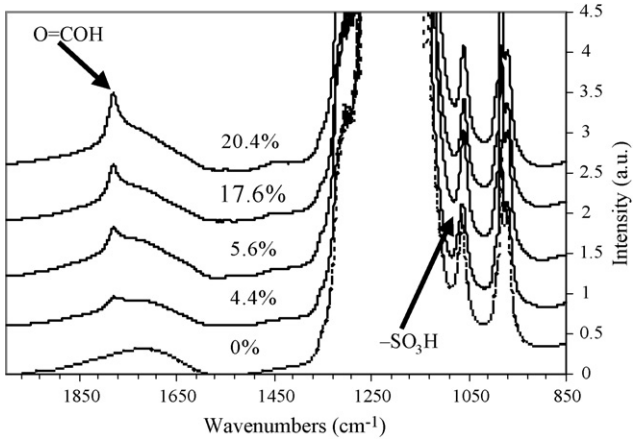

Fig. 4. FTIR transmission spectra of composite membranes. Spectra are stacked for comparison and bulk carboxylate content (%) is indicated above each spectrum.

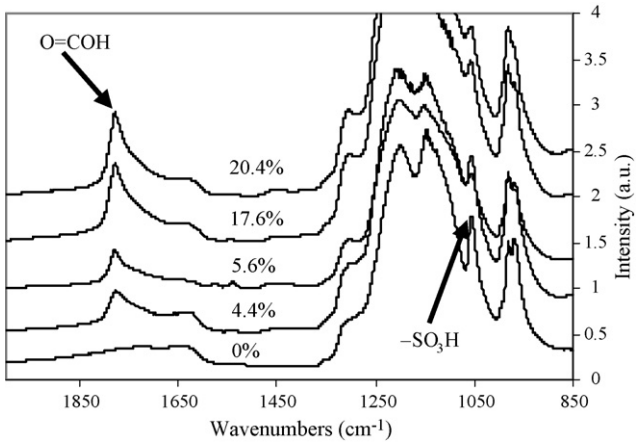

Fig. 5. FTIR ATR spectra of composite membranes. Spectra are stacked for comparison and bulk carboxylate content (%) is indicated above each spectrum.

$\sim$1060 cm^{-1}. The ATR spectra, in comparison, show a strong absorption at $\sim$1785 cm^{-1} for all composites, and a uniform absorption at $\sim$1060 cm^{-1}, which is considerably smaller than the corresponding peak in hydrolyzed precursor. Since ATR measurements probe the surface of the film while transmission measurements sample the bulk of the film, it is evident that the surfaces of the films have a high concentration of carboxylic acid while the bulk of the film probably contains a lower concentration. This implies a layered membrane, with two composite carboxylate/sulfonate outer layers and a sulfonate, Nafion®-like center.

The relationship between proton conductivity and water permeability in the composite films is shown in Figs. 6 and 7. As Fig. 6 illustrates, both proton conductivity and water permeability are quite low above 30% carboxylate substituted equivalents, which indicates that the carboxylic acid moieties effectively restrict the mobility of protons and water in the membrane. This is consistent with other studies which have shown a very poor proton conductivity in carboxylate form Nafion® [2]. Below 30% carboxylate, the composite membranes' performance is more interesting. As carboxylate content increases, proton conductivity decreases proportionally and water permeability decreases exponentially. This result is also shown in Fig. 7, where proton conductivity is plotted versus water permeability on a semi-log scale. Clearly, there is a relationship between the two quantities, with the proton conductivity affected less than the water permeability as the carboxylic acid concentration increases.

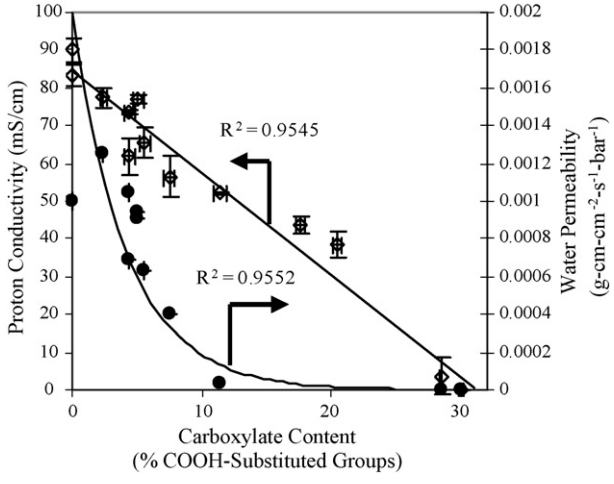

Fig. 6. Proton conductivity and water permeability in composite membranes. The line through the conductivity data is a linear least-squares regression and the line though the permeability data is an exponential least-squares regression.

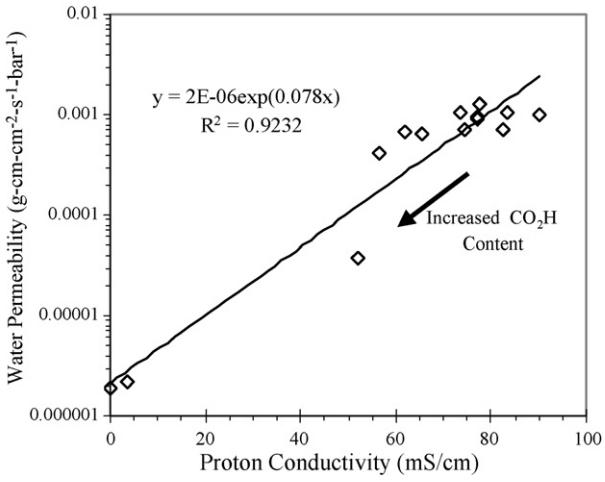

Fig. 7. Proton conductivity and water permeability in composite membranes. The line through the data is an exponential least-squares regression.

Equilibrium water sorption in the composite membranes is shown in Fig. 8. For composites with less than 20% carboxylate equivalents, water sorption is nearly uniform, with a slight decrease occurring toward higher carboxylate contents. It is known that carboxylate ionomers absorb less water than sulfonate ionomers [2,6,45], so a steady decrease in water content with increased carboxylate functionality would be expected. The high water sorption at moderate carboxylate content, therefore, is unexpected and will be discussed further below. Fig. 9 shows the relationship between proton conductivity and equilibrium water sorption in the composites. In general, membranes with high water content have a high conductivity, but there is no clear relationship between water sorption and conductivity in the composite films.

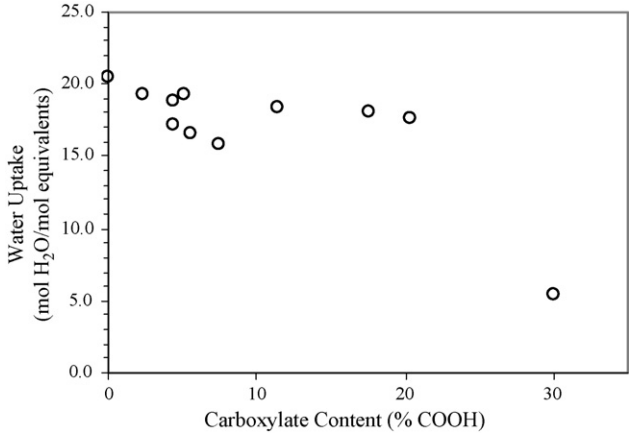

Fig. 8. Room temperature liquid water sorption by composite membranes.

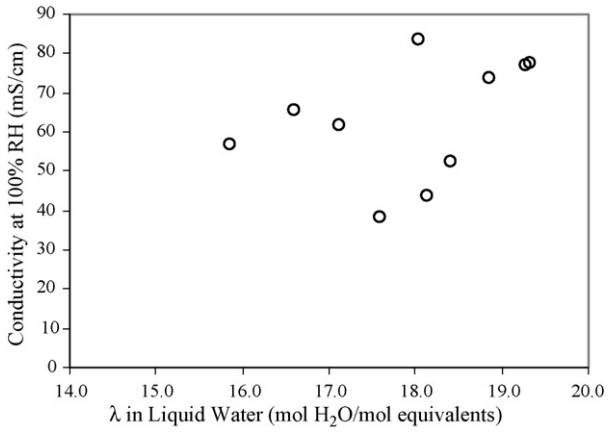

Fig. 9. Relationship between water sorption and conductivity in composite membranes.

Fig. 10 shows total flux and selectivity data for methanol/water solutions. In contrast with Figs. 6 and 7, Fig. 10a compares total flux through composites instead of permeability to avoid any ambiguity that may be raised from the pervaporation of a liquid mixture through Nafion®. As carboxylate content is increased, total flux decreases. Further, at low carboxylate content, the total flux increases with higher temperature and methanol concentration, but becomes increasingly independent

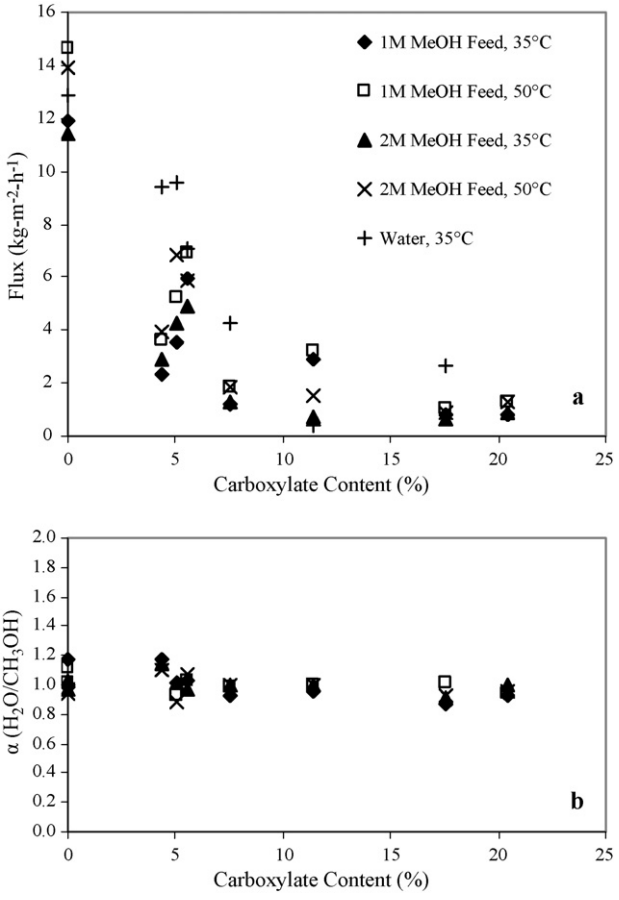

Fig. 10. Total methanol and water flux (a), and water/methanol selectivity (b) in composite membranes. Error bars are not pictured since their magnitudes are much lower than the scale of the plots.

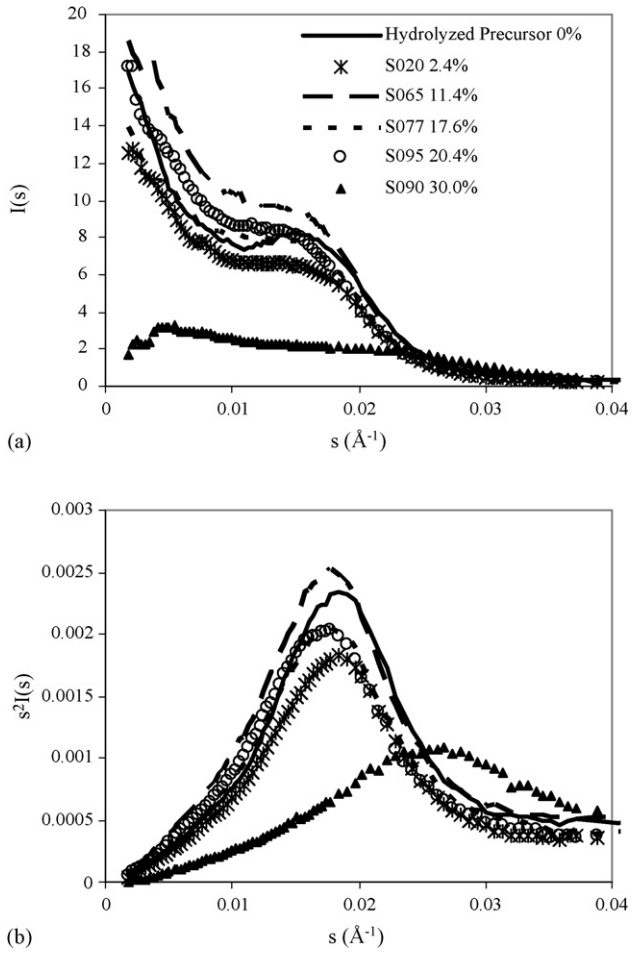

Fig. 11. (a) SAXS data for composite membranes and (b) multiplied by s^2 to show the position of the scattering maximum more clearly.

of heat or feed composition at higher carboxylate content. Under the conditions studied, the flux of pure water is higher than the total flux of methanol solution in many films. There is no preferential permeation of water or methanol in any composite (Fig. 10b).

Results from room temperature SAXS studies are shown in Fig. 11, both as raw SAXS intensity and as intensity multiplied by the square of the reciprocal lattice vector. For all membranes considered, less the 30% carboxylate sample, the SAXS profiles show a scattering maximum at $s \sim 0.018\ \text{Å}^{-1}$, which is associated with hydrated ionic domains [42]. In the 30% CO_2H sample, this scattering maximum lies at $s \sim 0.026\ \text{Å}^{-1}$. Fujimura et al. [42] showed that carboxylate form Nafion® membranes do not exhibit an ionic scattering maximum. Fig. 11, however, shows that for composite membranes with at least 30% carboxylate substituted equivalents, the ionic scattering maximum does not disappear. In fact, this maximum does not shift or weaken in intensity below 20% carboxylate, indicating that the size of the ionic domains does not change with small substitutions of carboxylic acid. Table 2 gives the average sizes of hydrated ionic domains in the composite membranes, as well as data from several Nafion® membranes. It is clear from the table that substitution of carboxylic acid for sulfonic acid in small amounts does not significantly alter the morphology of the membrane.

Table 2
Average size of hydrophilic domains in composite carboxylate/sulfonate and Nafion® membranes from SAXS and Eq. (10)

Membrane	Carboxylate content (%)	Average size or separation of ionic domains ($Å^{-1}$)
Nafion 112	0	53
Nafion 115	0	58
Nafion 117	0	48
Hydrolyzed precursor	0	54
S020.75w.HL	2.4	55
S070.75w.HL	7.5	53
S065.75w.HL	11.4	56
S077.75w.HL	17.6	56
S095.75w.HL	20.4	57
S090.100.H	30.0	38

4. Discussion

The results shown in Figs. 6 and 7 suggest that proton conduction in the composite films is occurring via the two classical mechanisms: by Grotthuss proton hopping and as hydrated cations, the so-called vehicle mechanism. If protons were moving though the ionomer as hydrated ions only, the conductivity would scale with permeability; i.e. if water mobility were significantly reduced in the membrane, proton movement would be as well. Conversely, if protons were moving through the ionomer by "jumping" between fixed water and anions, the conductivity would be independent of water permeability; i.e. the presence of water in the membrane would be sufficient for proton conduction, regardless of its mobility. The fact that water permeability drops sharply with a less dramatic decrease in conductivity may indicate a shift in the primary conduction mechanism to a larger Grotthuss-type contribution. Kreuer has given an in-depth discussion of the mechanisms of long-range proton transport [23], noting that proton mobility requires proton transfer reactions within hydrogen bonds and structural reorganizations of protonated molecules (water in this case) in non-metallic systems. In the presence of short, strong hydrogen bonds, rapid proton transfer is favored. The presence of shorter, stronger hydrogen bonds is expected in carboxylic acid-rich regions of the composites, since they are less acidic than sulfonic acid regions and apt to hydrogen bond with water [45]. Therefore, based on Kreuer's discussion, it is reasonable to expect a decreased mobility of water and an enhancement of Grotthuss proton hopping in the composites. This in turn explains the behavior shown in Figs. 6 and 7: water permeability decreases as it is increasingly "bound" by carboxylic acid groups while proton conductivity remains high, minus losses due to the lower acidity of carboxylic acids (less proton donating ability) and the higher activation energy associated with proton hopping as compared to hydronium ion diffusion [23].

The results in Fig. 8, in conjunction with the results in Figs. 6 and 7 are further proof that the carboxylate moieties alter the mass transfer characteristics of Nafion membranes®. Zawodzinski et al. and Meier and Eigenberger have shown that as water content decreases in Nafion®, water diffusion and hence permeability decreases in kind [22,35]. Therefore, we would expect a large decrease in permeability in the composites *if* the water content decreased significantly, which it does not. Eq. (4) states that at constant water content, the permeability should only decrease if the diffusivity decreases. Since the water content in composite films is nearly constant at low carboxylate content, Figs. 6–8 are evidence that the diffusivity of water is greatly reduced by the presence of a weaker acid.

Considering proton conductivity, it is clear that the composite films do not follow trends typically seen in Nafion®. Zawodzinski et al. [46] showed that as water content increases in Nafion®, conductivity increases proportionally. Composite membranes, in contrast, exhibit no clear relationship between these quantities. This indicates that the reduced conductivity must be due to interactions between water, protons, and the carboxylic acid (such as differences in solvation of carboxylate versus sulfonate, hydrogen bonding strengths, etc.), and not due to changes in water content.

The methanol and water data in Fig. 10 are both intriguing and anticlimactic, depending on how they are approached. While composites show a similar trend in total flux versus carboxylate content at each methanol concentration and temperature, it is remarkable to see that the flux of pure water at 35 °C is typically higher than that of 2 M methanol at 50 °C. Villaluenga et al. [47] showed that under identical hydraulic pressure driving forces, the total fluxes of methanol solutions were higher than the flux of pure water in Nafion® 117. Ren et al. [10] showed that up to a concentration of 10 M methanol, water uptake in Nafion® remains constant, with additional swelling due to methanol. Assuming the composites imbibe methanol and water in similar proportions as Nafion, it is expected that methanol solutions will increase total sorption in the films, leading to increased total fluxes. The fact that the opposite is observed suggests that the carboxylic acids may restrict further swelling from methanol, interact with methanol and water in a synergistic fashion that leads to a decrease in solvent diffusivity (through hydrogen bonding, as one possibility), or both. Of course, Fig. 10b shows that water and methanol are equally restricted by the carboxylate moieties, which means that there is no particular carboxylate/methanol interaction responsible for the decreased overall flux. Kawamura et al. [48] and Ren et al. [49] showed that methanol solutions partition equally into Nafion®. Therefore, the lack of separation by composite membranes should not be surprising.

The SAXS results indicate that composites with small amounts of carboxylate form ionic 'clusters' similar in size to those in Nafion®, while films with high carboxylate content do not. This is probably why the composite membranes behave very differently than carboxylate form Nafion®, exhibiting proton conductivities of the same order of magnitude as N111. Qualitatively, the SAXS data are consistent with the swelling data, in that neither the water sorption nor the position and intensity of the ionic scattering maximum change appreciably at low carboxylate content. At high carboxylate content, the scattering maximum shifts and lowers in intensity and the water content drops. This in turn is in agreement with the literature, where many authors have shown a decreased water content coupled with a shift of the ionic scattering maximum to higher *s*

and a decrease in peak intensity (due to smaller domain sizes) [33,39–42].

For fuel cell applications, a shift in the contributions from proton conduction mechanisms from vehicle-type to Grotthuss-type, as hypothesized above, has several implications. First, a smaller inventory of water would be needed in the electrolyte to maintain high proton conductivity, due to decreased dehydration of the ionomer caused by electroosmotic drag. Second, water involved in strong hydrogen bonds (with better proton transfer ability) would be more difficult to remove from the ionomer, mitigating the harsh drying effect at elevated temperatures. Third, the decreased movement of water through the membrane would reduce the overall co-transport of water and methanol through the membrane, reducing total methanol crossover, and improving the performance of the DMFC.

It must be noted that the importance of this study is not to find better electrolyte materials for fuel cell applications through the addition of carboxylate anions, but to understand what types of chemical modifications will improve the PEM in high temperature operation and in DMFCs. In fact, it is believed that Nafion® membranes degrade through a radical depolymerization, which is initiated with peroxy radicals and trace carboxylic acid groups in the film [5,50]. At elevated temperatures, this degradation will occur at an increased rate. Replacement of sulfonic acid groups with carboxylic acid groups, therefore, should speed the decomposition of Nafion® in fuel cell environments.

It is hoped that this study will show the benefit of using proton conductivity and water permeability measurements as a prescreening tool for advanced fuel cell electrolytes. One should suspect that low water permeability coupled with high proton conductivity could translate to decreased methanol crossover in DMFCs and less-severe dehydration in H_2/O_2 fuel cells. And, because these measurements are quick and inexpensive, the researcher stands to save time and money in *not* testing all experimental membranes in a fuel cell. There are drawbacks to prescreening membrane samples in this fashion, however, namely that the membranes are only tested under conditions of saturated vapor or liquid. In an operating fuel cell, the electrolyte will be required to perform under conditions of low humidity and high temperature. Further, conductivity and permeability tests do not take into account the coupled nature of mass and proton transport, as they isolate the two by themselves. To expand the scope of information obtained using these two methods, the interested researcher can measure conductivities using methods in this study, and water permeabilities using a combination of the pervaporation system described here and the feed system used by Thomas et al. [33], at different temperatures and relative humidities.

As a final note, it must be realized that the quantities measured above are averaged values, and may not represent transport behavior in the composite membranes on a local level. For instance, conductivity may be poor near the surfaces and high in the center of the films, averaging to an overall conductivity that is slightly reduced from Nafion® 111. Similarly, the water permeability, swelling, and local microstructure may average to values near those for Nafion®, while small regions of the film could experience low water sorption and permeability, affecting the overall performance of the membrane. Therefore, to be sure that proton and water transport mechanisms are different in composite films, they will be tested in real H_2/O_2 and direct methanol fuel cell environments over a range of conditions. The results of said study will be reported in a later publication.

5. Conclusions

Composite perfluorinated carboxylate/sulfonate ionomer membranes were prescreened for fuel cell suitability via proton conductivity and water permeability tests. Addition of the carboxylic acid functional group dramatically reduced the water permeability and modestly reduced the proton conductivity in the films, suggesting a change in the proton conduction mechanism toward more Grotthuss-type movement (compared to Nafion®). This could have implications of reduced electrolyte dehydration in fuel cell operation and/or decreased methanol crossover in DMFCs. SAXS analysis showed that composites with up to 20% carboxylate equivalents have hydrated ionic domains similar in size to those in Nafion. Water sorption measurements showed little decrease in water uptake with increased carboxylate functionality, supporting the SAXS data. When compared to water permeability, the water sorption results show evidence that water may be more tightly held in composite films than in Nafion®. Methanol/water permeability and selectivity measurements showed that the composite membranes provide no permselectivity of water over methanol, but do decrease the permeability of both species. It is proposed that permeability and conductivity measurements could provide an inexpensive and simple screening tool for early evaluation of new experimental proton exchange membranes.

Acknowledgements

Funding for this project is provided by the Dept. of Energy through the Los Alamos National Laboratory, under subcontract number 16063-001-05. LANL is operated by the University of California under Contract No. W-7405-ENG-36. Additional financial support was provided by grant DE-FG03-93ER14363 from the DOE office of science, Basic Energy Sciences Program, Chemical Sciences Division. The authors would like to thank Dr. Colin Wolden of CSM for use of his potentiostat, Dr. Don Williamson of CSM for running the small angle X-ray instrument, Cole Reeder for help around the laboratory, and Drs. Andy Herring of CSM, Steve Hamrock of 3M, and Drs. Marc Doyle and Dennis Curtin of DuPont for useful discussions. Finally, we wish to thank DuPont Fuel Cells for providing fresh Nafion® 111-F precursor material, which has proven critical to the success of our research.

References

[1] T. Schultz, K. Sundmacher, S. Zhou, Chem. Eng. Technol. 24 (2001) 1223–1233.
[2] M. Doyle, R.G. Rajendran, in: W. Vielstich, A. Lamm, H.A. Gastreiger (Eds.), Handbook of Fuel Cells, Fundamentals Technology and Applications, John Wiley & Sons, Ltd., Chichester, 2003, pp. 351–395.
[3] K. Ramya, K.S. Dhathathreyan, J. Electroanal. Chem. 542 (2003) 109–115.

[4] N. Jia, M.C. Lefebvre, J. Halfyard, Z. Qi, P.G. Pickup, Electrochem. Solid State 3 (2000) 529–531.
[5] A.M. Herring, Encyclopedia of Chemical Processing, Taylor and Francis, 2006, pp. 1085–1097.
[6] K.A. Mauritz, R.B. Moore, Chem. Rev. 104 (2004) 4535–4585.
[7] A.M. Herring, J. Macromol. Sci. R.M.C. 46 (2006) 245–296.
[8] B.S. Pivovar, Y. Wang, E.L. Cussler, J. Membr. Sci. 154 (1999) 155–162.
[9] B. Ruffmann, H. Silva, B. Schulte, S.P. Nunes, Solid State Ionics 162–163 (2003) 269–275.
[10] X. Ren, T.E. Springer, S. Gottesfeld, J. Electrochem. Soc. 147 (2000) 92–98.
[11] H. Wang, B.A. Holmberg, L. Huang, Z. Wang, A. Mitra, J.M. Norbeck, Y. Yan, J. Mater. Chem. 12 (2002) 834–837.
[12] R.G. Rajendran, MRS Bull. 30 (2005) 587–590.
[13] M. Doyle, S.K. Choi, G. Proulx, J. Electrochem. Soc. 147 (2000) 34–37.
[14] Q. Li, R. He, J.O. Jensen, N.J. Bjerrum, Chem. Mater. 15 (2003) 4896–4915.
[15] M. Watanabe, H. Uchida, Y. Seki, M. Emori, P. Stonehart, J. Electrochem. Soc. 143 (1996) 3847–3852.
[16] X. Li, E.P.L. Roberts, S.M. Holmes, J. Power Sources 154 (2006) 115–123.
[17] P. Dimitrova, K.A. Friedrich, U. Stimming, B. Vogt, Solid State Ionics 150 (2002) 115–122.
[18] A. Sungpet, J. Membr. Sci. 226 (2003) 131–134.
[19] T. Arimura, D. Ostrovskii, T. Okada, G. Xie, Solid State Ionics 118 (1999) 1–10.
[20] M. Alvaro, A. Corma, D. Das, V. Fornés, H. Garcia, Chem. Commun. (2004) 956–957.
[21] Y.J. Kim, W.C. Choi, S.I. Woo, W.H. Hong, J. Membr. Sci. 238 (2004) 213–222.
[22] T.A. Zawodzinski, C. Derouin, S. Radzinski, R.J. Sherman, V.T. Smith, T.E. Springer, S. Gottesfeld, J. Electrochem. Soc. 140 (1993) 1041–1047.
[23] K.D. Kreuer, Solid State Ionics 136–137 (2000) 149–160.
[24] T.A. Zawodzinski, J. Davey, J. Valerio, S. Gottesfeld, Electrochim. Acta 40 (1995) 297–302.
[25] X. Ren, S. Gottesfeld, J. Electrochem. Soc. 148 (2001) A87–A93.
[26] T.A. Zawodzinski, T.E. Springer, F. Uribe, S. Gottesfeld, Solid State Ionics 60 (1993) 199–211.
[27] D.R. Morris, X. Sun, J. Appl. Polym. Sci. 50 (1993) 1445–1452.
[28] T. Okada, G. Xie, O. Gorseth, S. Kjelstrup, N. Nakamura, T. Arimura, Electrochim. Acta 43 (1998) 3741–3747.
[29] R.L. Ames, J.D. Way, E.A. Bluhm, D.M. Knauss, R.P. Singh, J.E. Hensley, Ind. Eng. Chem. Res. 44 (2005) 3672–3680.
[30] W.G. Grot, C.J. Molnar, P.R. Resnick, US Patent 4,544,458 (1985).
[31] R.L. Ames, Nitric Acid Dehydration Using Perfluoro Carboxylate and Mixed Sulfonate/Carboxylate Membranes, Colorado School of Mines, Golden, 2004.
[32] J.G. Wijmans, R.W. Baker, J. Membr. Sci. 79 (1993) 101–113.
[33] M. Thomas, M. Escoubes, P. Esnault, M. Pineri, J. Membr. Sci. 46 (1989) 57–65.
[34] X. Ye, M.D. LeVan, J. Membr. Sci. 221 (2003) 147–161.
[35] F. Meier, G. Eigenberger, Electrochim. Acta 49 (2004) 1731–1742.
[36] K.D. Kreuer, J. Membr. Sci. 185 (2001) 29–39.
[37] J.T. Hinatsu, M. Mizuhata, H. Takenaka, J. Electrochem. Soc. 141 (1994) 1493–1498.
[38] M. Doyle, M.E. Lewittes, M.G. Roelofs, S.A. Perusich, R.E. Lowrey, J. Membr. Sci. 184 (2001) 257–273.
[39] G. Gebel, Polymer 41 (2000) 5829–5838.
[40] J.T. Wescott, Y. Qi, L. Subramanian, T.W. Capehart, J. Chem. Phys. 124 (2006) 1–14.
[41] T.D. Gierke, G.E. Munn, F.C. Wilson, J. Polym. Sci. 19 (1981) 1687–1704.
[42] M. Fujimura, T. Hashimoto, H. Kawai, Macromolecules 14 (1981) 1309–1315.
[43] S.A. Perusich, Macromolecules 33 (2000) 3431–3440.
[44] C. Heitner-Wirguin, Polymer 20 (1979) 371–374.
[45] H.L. Yeager, Z. Twardowski, L.M. Clarke, J. Electrochem. Soc. 129 (1982) 324–327.
[46] T.A. Zawodzinski, M. Neeman, L.O. Sillerud, S. Gottesfeld, J. Phys. Chem. (US) 95 (1991) 6040–6044.
[47] J.P.G. Villaluenga, B. Seoane, V.M. Barragán, C. Ruiz-Bauzá, J. Colloid Interf. Sci. 268 (2003) 476–481.
[48] J. Kawamura, K. Hattori, T. Hongo, R. Asayama, N. Kuwata, T. Hattori, J. Mizusaki, Solid State Ionics 176 (2005) 2451–2456.
[49] X. Ren, T.E. Springer, T.A. Zawodzinski, S. Gottesfeld, J. Electrochem. Soc. 147 (2000) 466–474.
[50] D.E. Curtin, R.D. Lousenburg, T.J. Henry, P.C. Tangeman, M.E. Tisack, J. Power Sources 131 (2004) 41–48.